THE JOURNAL OF BIOLOGICAL CHEMISTRY
Vol. 280, No. 15, Issue of April 15, pp. 14645–14655, 2005
Printed in U.S.A.
© 2005 by The American Society for Biochemistry and Molecular Biology, Inc.

The Skp1 Prolyl Hydroxylase from *Dictyostelium* Is Related to the Hypoxia-inducible Factor-α Class of Animal Prolyl 4-Hydroxylases*

Received for publication, January 18, 2005, and in revised form, February 7, 2005
Published, JBC Papers in Press, February 10, 2005, DOI 10.1074/jbc.M500600200

Hanke van der Wel, Altan Ercan, and Christopher M. West‡

From the Department of Biochemistry and Molecular Biology, Oklahoma Center for Medical Glycobiology, University of Oklahoma Health Sciences Center, Oklahoma City, Oklahoma 73104

Skp1 is a cytoplasmic and nuclear protein of eukaryotes best known as an adaptor in SCF ubiquitin-protein isopeptide ligases. In *Dictyostelium*, Skp1 is subject to 4-hydroxylation at Pro^{143} and subsequent *O*-glycosylation by α-linked GlcNAc and other sugars. Soluble cytosolic extracts have Skp1 prolyl 4-hydroxylase (P4H) activity, which can be measured based on hydroxylation-dependent transfer of [^{3}H]GlcNAc to recombinant Skp1 by recombinant (Skp1-protein)-hydroxyproline α-*N*-acetyl-D-glucosaminyltransferase. The *Dictyostelium* Skp1 P4H gene (*phyA*) was predicted using a bioinformatics approach, and the expected enzyme activity was confirmed by expression of *phyA* cDNA in *Escherichia coli*. The purified recombinant enzyme (P4H1) was dependent on physiological concentrations of O_2, α-ketoglutarate, and ascorbate and was inhibited by $CoCl_2$, 3,4-dihydroxybenzoate, and 3,4-dihydroxyphenyl acetate, as observed for known animal cytoplasmic P4Hs of the hypoxia-inducible factor-α (HIFα) class. Overexpression of *phyA* cDNA in *Dictyostelium* yielded increased enzyme activity in a soluble cytosolic extract. Disruption of the *phyA* locus by homologous recombination resulted in loss of detectable activity in extracts and blocked hydroxylation-dependent glycosylation of Skp1 based on molecular weight analysis by SDS-PAGE, demonstrating a requirement for P4H1 *in vivo*. The sequence and functional similarities of P4H1 to animal HIFα-type P4Hs suggest that hydroxylation of Skp1 may, like that of animal HIFα, be regulated by availability of O_2, α-ketoglutarate, and ascorbate, which might exert novel control over Skp1 glycosylation.

Skp1 is a subunit of the SCF (Skp1-cullin-F box protein complex) class of ring finger ubiquitin-protein isopeptide ligases (E3),[1] which are involved in the polyubiquitination of selected, usually phosphorylated proteins for degradation (1). Many proteins have been identified as substrates for these ligases, including cell division kinase inhibitors, transcription factor subunits, and a cytoplasmic cAMP phosphodiesterase in *Dictyostelium* (2). In the SCF complex, Skp1 serves as an adaptor linking the F box protein, a member of a family of target recognition proteins, and the cullin-1/Rbx1 dimer, which in turn binds the catalytic ubiquitin carrier protein (3). The exact function of Skp1 is not known, but it may regulate assembly of the SCF complex (*e.g.* Ref. 4). Co-immunoprecipitation and two-hybrid studies have suggested that Skp1 is a multifunctional protein that also participates in other cellular processes (5, 6).

In *Dictyostelium*, a soil ameba in the mycetozoan group of unicellular eukaryotes, Skp1 is post-translationally modified by an unusual pentasaccharide that is linked to hydroxylated Pro^{143} (7). Glycosylation is mediated by the sequential action of soluble cytoplasmic glycosyltransferases (8). The gene for the first glycosyltransferase in the pathway, (Skp1 protein)-hydroxyproline α-*N*-acetyl-D-glucosaminyltransferase (GnT1) (9), is evolutionarily related to animal polypeptide α-GalNAc-transferases, which initiate mucin-type *O*-glycosylation in the Golgi apparatus (10–12). The next two sugars are attached by a bifunctional diglycosyltransferase with β-3-galactosyltransferase and α-2-fucosyltransferase activities (13). The catalytic domains of the diglycosyltransferase are each related to separate families of cytoplasmically associated glycosyltransferase domains of bacteria and eukaryotes (12). The next sugar, α-3-linked Gal, is attached by a separate soluble enzyme (14). The final glycan formed consists of a type 1 blood group H structure with peripheral α-linked Gal modifications: Galα1,Galα1,-3Fucα1,2Galβ1,3GlcNAcα1-.

The first sugar, GlcNAc, is likely to be α-linked to the 4-position of Hyp based on homology between GnT1 and known retaining glycosyltransferases (12) and because a synthetic peptide with a 4-OH substituent on the target Pro residue is a good acceptor substrate for GnT1 (15). Pro^{143} hydroxylation, which because of hydroxylation-dependent glycosylation can be monitored *in vivo* by molecular weight shift analysis of extracts by SDS-PAGE (16), is inhibited by α,α′-dipyridyl and ethyl 3,4-dihydroxybenzoate, suggesting the involvement of a collagen-type or hypoxia-inducible factor (HIF)-1α-type prolyl 4-hydroxylase (P4H). Collagen-type P4Hs coordinate Fe^{2+} in their active sites using two critical His residues, a Glu/Asp residue, α-ketoglutarate, and O_2 and catalyze the coupled cleavage of O_2 with decarboxylation of α-ketoglutarate and 4-hydroxylation of the target Pro residue (17). Ascorbate is also essential possibly for maintaining the oxidation state of iron. Because collagen P4Hs reside in the lumen of the rough endoplasmic reticulum and because Skp1 appears to be processed in the cytoplasm, the recently described members of the cytoplasmic HIF1α P4H family (18, 19) are also candidates for Skp1 hydroxylation. HIF1α is a transcription factor subunit that is constitutively hydroxylated by one or more of the three known mammalian enzymes (PHD or HPH) at two separate Pro residues, which

* This work was supported in part by National Institutes of Health Grant R01-GM37539. The costs of publication of this article were defrayed in part by the payment of page charges. This article must therefore be hereby marked "*advertisement*" in accordance with 18 U.S.C. Section 1734 solely to indicate this fact.

The nucleotide sequence(s) reported in this paper has been submitted to the GenBank™/EBI Data Bank with accession number(s) AY768817.

‡ To whom correspondence should be addressed: Dept. of Biochemistry and Molecular Biology, University of Oklahoma Health Sciences Center, 940 Stanton L. Young Blvd., BMSB 937, Oklahoma City, OK 73104. Tel.: 405-271-2227 (ext. 1247); Fax: 405-271-3139; E-mail: Cwest2@ouhsc.edu.

[1] The abbreviations used are: E3, ubiquitin-protein isopeptide ligase; GnT1, (Skp1 protein)-hydroxyproline α-*N*-acetyl-D-glucosaminyltransferase; HIF, hypoxia-inducible factor; P4H, prolyl 4-hydroxylase; VHL, von Hippel-Lindau; r, recombinant; mAb, monoclonal antibody; TEV, tobacco etch virus.

This is an Open Access article under the CC BY license.

leads to their recognition by von Hippel-Lindau (VHL) protein E3 and subsequent polyubiquitination and proteasomal degradation (20, 21). If cells are limited for any of the P4H substrates or cofactors, including O_2, α-ketoglutarate, ascorbate, and Fe^{2+} (18, 19, 22, 23), hydroxylation diminishes, and HIF1α accumulates, dimerizes with HIF1β, enters the nucleus, and directly induces the expression of a set of hypoxia-related genes. This appears to be an important pathway of O_2 sensing in invertebrate and vertebrate animal cells (24).

Glycosylation of Skp1 is required for its concentration in the nucleus and also appears to influence cell size and maximal cell density in axenic media (8). Prolyl hydroxylation is required for Skp1 glycosylation (16) and might regulate this post-translational modification. To investigate this possibility further, the fully sequenced *Dictyostelium* genome was scanned for sequences containing the critical Fe^{2+}-coordinating amino acid triad and other P4H motifs using BLAST (25). Five candidate coding regions predicted to encode cytoplasmic proteins were identified (12). These sequences are diverse based on phylogenetic analysis of P4H-like sequences from many organisms. A similar search in the genomes of the diatom *Thalassiosira pseudonana* and the oomycete *Phytophthora sojae* identified, in each, a novel candidate bifunctional gene predicted to encode both P4H activity and Skp1 α-GlcNAc-transferase activity. The *Dictyostelium* sequence most closely related to the diatom and oomycete P4H-like sequence, implicated in the Skp1 modification pathway by its association with an Skp1 GnT1-like sequence, was also the most closely related of the five to the HIFα class of animal P4H sequences. This gene, referred to as *phyA*, is shown here to encode Skp1 P4H based on its biochemical activity and its requirement for Skp1 glycosylation *in vivo*. This finding in the model system *Dictyostelium* suggests that HIFα P4Hs are an ancient enzyme family that had its evolutionary origins in lower eukaryotes or even prokaryotes and opens new lines of studies into O_2 and metabolite regulation of cell physiology in microbes, including parasites and pathogens of plants and animals.

EXPERIMENTAL PROCEDURES

Dictyostelium Cell Culture—Dictyostelium strain Ax3 and its derivatives were passaged axenically in HL-5 medium or on SM agar in the presence of *Klebsiella aerogenes* as described (16). Cell density was determined using a hemacytometer. Cells were grown to stationary phase, *i.e.* maximal density (2×10^7 cells/ml), for extraction and assays.

Skp1 P4H Activity Assay—Skp1 P4H activity was detected using a coupled assay in which the product of the P4H reaction, Skp1 hydroxylated at Pro^{143}, was detected by subsequent addition of [^{3}H]GlcNAc in the presence of GnT1, the second enzyme in the Skp1 modification pathway. The standard one-step reaction mixture (adapted from Refs. 15, 26, and 27 and optimized as described here) contained 50 mM Tris-HCl (pH 7.4), 5 μM $FeSO_4$, 1 mM ascorbic acid, 0.5 mM α-ketoglutarate, 5 mM dithiothreitol, 0.2 mg/ml catalase (Sigma), 10 mM $MgCl_2$, 0.02% (v/v) Tween 20, 1 μM UDP-[^{3}H]GlcNAc (American Radiochemical Corp.; diluted to 20 Ci/mmol with unlabeled UDP-GlcNAc from Sigma), 0.9 μM recombinant (r) Skp1 (see below), rGnT1 (see below), and the P4H preparation in a volume of 50 μl. Assays of crude cell extracts also contained 1 mM ATP and 3 mM NaF. Assays of highly purified His_6-rP4H contained 0.15 μg of enzyme protein as estimated from Coomassie Blue-stained material on SDS-polyacrylamide gels. The reaction was incubated at 29 °C for 1–3 h. Incorporation of [^{3}H]GlcNAc into rSkp1 was analyzed either as trichloroacetic acid precipitates recovered on GF/C filters, followed by liquid scintillation spectrometry in BioSafe NA (Research Products International Corp.), or by SDS-PAGE, excision of slices at the position of rSkp1, and counting in gel scintillation mixture as described (15).

In some cases, P4H was assayed in two steps. The initial reaction volume (50 μl) contained 50 mM Tris-HCl (pH 7.4), 5 μM $FeSO_4$, 2 mM ascorbic acid, 0.5 mM α-ketoglutarate, 0.3 mM dithiothreitol, 0.2 mg/ml catalase, 0.9 μM rSkp1, and the P4H fraction. After 2 h at 29 °C, the reaction volume was increased to 60 μl to contain 50 mM Tris-HCl (pH 7.4), 5 mM dithiothreitol, 10 mM $MgCl_2$, 0.02% Tween 20, 1 μM UDP-GlcNAc (see above), and rGnT1 in addition to the diluted solutes from the first step and was incubated for an additional 2 h.

To determine O_2 dependence, reactions were conducted in 1-ml conical bottom Reacti-Vials (Pierce) under a continuously flowing atmosphere of compressed gas provided by piercing rubber septa in the caps with syringe needles fitted with plastic tubing. Compressed gasses of different percentages of O_2 ($\pm$2% by measurement) in N_2 were prepared commercially (Airgas-MidSouth, Tulsa, OK) and bubbled through an in-line water reservoir before use. 21% O_2 was provided from a compressed air source, as the reaction conducted under ambient atmosphere without flow or agitation yielded a lower value, indicating O_2 starvation. The reactions were carried out for 0 or 1 h.

Skp1 GlcNAc-transferase Activity Assay—Activity was assayed as described previously using mutant Skp1A1-Myc isolated from *Dictyostelium* strain HW120 as the acceptor substrate (15).

rSkp1—Two isoforms of rSkp1 were produced in *Escherichia coli* harboring expression plasmids containing the *Dictyostelium* Skp1A coding region (28). His_{10}-rSkp1A contains an N-terminal His_{10} tag and was purified to near homogeneity as described (29). rSkp1A(P143A) consists of the native sequence of *Dictyostelium* Skp1A (28) except for the replacement of Pro^{143} with Ala. rSkp1A(P143A) was produced by ligation of the full-length coding region of Skp1A (amplified by PCR from the His_{10}-Skp1A plasmid using primers with AflIII and BamHI sites near their 5′ termini) into the NcoI and BamHI sites of pET19b (Novagen). The P143A substitution was created by site-directed mutagenesis (16). The resulting plasmid was transformed into chemically competent *E. coli* strain BL21-Gold(DE3) (Novagen). Clonal transfectants were grown in LB medium containing 100 μg/ml ampicillin at 37 °C on a shaker until an A_{590} (1-cm path length) of 0.4–0.6 was attained. Expression was induced by continued shaking in 0.5 or 1 mM isopropyl 1-thio-β-D-galactopyranoside (Research Products International Corp.) for 15 h at room temperature. Cells were cooled on ice for 5 min, centrifuged at 5000 $\times$ *g* for 5 min at 4 °C, washed twice by resuspension and recentrifugation in cold 20 mM Tris-HCl (pH 8.0), and frozen at −80 °C. Frozen cell pellets were resuspended on ice in *E. coli* lysis buffer (0.1 M Tris-HCl (pH 8.2), 1 mg/ml lysozyme, 5 mM benzamidine, 0.5 μg/ml pepstatin A, 5 μg/ml aprotinin, 5 μg/ml leupeptin, and 0.5 mM phenylmethylsulfonyl fluoride) at 1 ml/25 ml of the original culture volume, lysed in a French pressure cell (15,000 p.s.i.), and centrifuged at 100,000 $\times$ *g* for 1 h. The supernatant was purified by successive chromatography over a DEAE-Sepharose fast flow anion exchange column and a phenyl-Sepharose fast flow (Hi-Sub) column (both from Amersham Biosciences) (14). The pool of Skp1 that eluted in the ascending ethylene glycol gradient was further purified and concentrated over a Source 15Q anion exchange column (Amersham Biosciences) eluted with an ascending gradient of NaCl in 25 mM NH_4Ac (pH 7.5), 5 mM $MgCl_2$, 15% (v/v) glycerol, 1 mM dithiothreitol, and protease inhibitors (10 μg/ml leupeptin, 10 μg/ml aprotinin, and 1 mM phenylmethylsulfonyl fluoride). SDS-PAGE and Western blotting using monoclonal antibody (mAb) 4E1 showed that rSkp1 was readily observed as one of several major Coomassie Blue-stained bands (data not shown).

rGnT1—rGnT1 was produced in *E. coli* transformed with pGnT51-CBD, which encodes the full-length coding region of Skp1 GlcNAc-transferase-1 fused to the C terminus of a chitin-binding domain via a self-cleaving intein linker. *E. coli* was induced and extracted as described above, and spontaneously cleaved rGnT1 was recovered from the retarded flow-through fraction of a DEAE-Sepharose fast flow column (15). This fraction was applied to a phenyl-Sepharose fast flow (Hi-Sub) column equilibrated in 20% $(NH_4)_2SO_4$ in 50 mM Tris-HCl (pH 7.5), 5 mM $MgCl_2$, 0.1 mM EDTA, 1 mM dithiothreitol, and protease inhibitors (see above). As observed for native GnT1 (15), rGnT1 eluted in a large volume at the end of a descending gradient to 0% $(NH_4)_2SO_4$ based on an activity assay (see below). This pool was concentrated 100-fold in a Centriprep 30 centrifugal concentrator (Amicon, Inc.), with an activity yield of 50%.

Purification of P4H from Dictyostelium—An S100 fraction from stationary phase cells was prepared and subjected to serial anion exchange and phenyl-Sepharose chromatography as described previously for GnT1 (15), except that the 60% $(NH_4)_2SO_4$ precipitation step was skipped. P4H was assayed using the two-step method described above.

Cloning P4H1 Genomic DNA—Primers PHF-S and PHF-AS, which included the putative start and stop codons respectively (*underlined* in Fig. 2), were used to amplify the coding part (including introns) of the P4H1 gene from CsCl-purified *Dictyostelium* genomic DNA based on standard procedures (30) using a 9:1 mixture of *Taq* (Eppendorf) and *Pfu* (Stratagene) DNA polymerases for 30 cycles at 94 °C for 45 s, 51–58 °C for 45 s, and 68 °C for 3 min, followed by one cycle at 68 °C, 7 min. The resulting DNA fragment was cloned into pCR4TOPO (Invitrogen), yielding pTOPOgPH1. pTOPOgPH1 was sequenced using the

M13(F) and M13(R) primers, which exactly confirmed the genomic sequence reported for chromosome 2 in the GenBank™/EBI Data Bank (accession number AC115612.2; nucleotides 87226–88296) and the primary model for this gene at dictyBase (dictyBaseID DDB0169393; available at www.dictybase.org).

Disruption of the Dictyostelium P4H1 Gene—pTOPOgPH1 was digested with BstBI, which cuts at position 535 of P4H1 (see Figs. 2 and 3). The *bsr* (blasticidin S resistance) cassette was released from plasmid pBsR519 (31) using ClaI. Both digests were electrophoresed on a 1% (w/v) SEAKEM GTG-agarose (BioWhittaker) gel, and linearized pTOPOgPH1 and the released *bsr* cassette were retrieved using a freeze-squeeze method (32) and EtOH-precipitated. Linearized pTOPOgPH was treated with shrimp alkaline phosphatase (Roche Applied Science) for 1 h at 37 °C, followed by inactivation at 65 °C for 20 min. The DNA fragments were ligated for 3 h at 22 °C using T4 DNA ligase (New England Biolabs Inc.), which was then inactivated at 65 °C for 10 min. The resulting plasmid, pTOPO-PH1-BsR, was expressed in TOP10 *E. coli* cells (Invitrogen) and digested with SpeI and NotI. The P4H1-BsR insert was gel-purified as described above and treated briefly with Bal-31 exonuclease (New England Biolabs Inc.) to remove terminal residues derived from pCR4TOPO, which improved transformation frequency (data not shown) (33). Bal-31 was inactivated by incubation at 65 °C for 10 min in the presence of 0.5 M EGTA, and the DNA was EtOH-precipitated and redissolved in 2 mM Tris-HCl (pH 8.0). Strain Ax3 cells were transformed by electroporation as described (34). Transformants were selected in 10 μg/ml blasticidin S (MP Biomedicals) in HL-5$^+$ medium. Cell lysates from clones were analyzed for modification of the P4H1 locus using PCR and primers PHF-S and PHF-AS.

Cloning P4H1 cDNA—The predicted full-length coding region corresponding to the genomic DNA described above was amplified by reverse transcription-PCR using total RNA from *Dictyostelium discoideum* strain Ax3 developed for 13 h to the slug stage as described (35). The first strand of DNA was synthesized using Moloney murine leukemia virus reverse transcriptase (New England Biolabs Inc.) and primer PHF-AS (see Fig. 2). DNA was then amplified by adding primer PHF-S using PCR as described above. The resulting cDNA was cloned into pCR4TOPO, yielding pTOPOcPH1 and sequenced as described above to confirm fidelity.

Overexpression of P4H1 in D. discoideum—P4H1 cDNA was amplified from pTOPOcPH1 using primers PHF-pVS (5′-GACT**GGTACC**GAAAATAAAATAAAAAAATGGATATTTCTAACTTACCCCCTCAC) and PHF-pVAS (5′-CA**AGATCT**ATAAATCCAAGTTGTAATTGCAATTCTT) (KpnI and BglII cloning sites are in boldface, and underlined regions correspond to terminal coding DNA) as described above and cloned into pCR4TOPO. After sequencing to ensure fidelity, the resulting plasmid was digested with KpnI and BglII, and the open reading frame was directionally cloned into a similarly digested preparation of *Dictyostelium* expression vector pVS (33), which removed the signal peptide encoded by pVS. This plasmid, pVS-P4H1, placed the P4H1 open reading frame under the control of the discoidin-1γ promoter and appended a C-terminal c-Myc epitope tag. pVS-P4H1 was electroporated into strain Ax3 cells, and transformants were selected using 10 μg/ml G418 sulfate (Research Products International Corp.) in HL-5$^+$ medium as described above. Cultures were grown through three passages in 20 or 120 μg/ml G418 and cloned by growth on *K. aerogenes* on SM media plates. S100 and P100 fractions were generated from cell lysates by ultracentrifugation at 100,000 × *g* for 60 min. For P4H assays, the S100 fraction was desalted on a 9-ml PD-10 column (Amersham Biosciences) containing Sephadex G-25 in 50 mM Tris-HCl (pH 7.4) with protease inhibitors (see above).

Expression and Purification of rP4H1 in E. coli—P4H1 cDNA was amplified from pTOPOcPH1 using primers PH1-pETS (5′-CA**CATATG**GATATTTCTAACTTACCCCCTCAC) and PH1-pETAS (5′-CA**GGATCC**TTAATAAATCCAAGTTGTAATTGCAATTCTT) (NdeI and BamHI sites are in boldface, and underlined regions correspond to terminal coding DNA) and cloned into pCR4TOPO. After sequencing to ensure faithful amplification, the cDNA was released by digestion with NdeI and BamHI and directionally cloned into similarly digested pET15TEVi (36). pET15TEVi was derived from pET15b (Novagen) by replacement of the thrombin cleavage site with a tobacco etch virus (TEV) protease cleavage site and a 320-nucleotide insert between the restriction enzyme sites (a gift of Dr. A. Bochkarev). The resulting *E. coli* expression plasmid, pET15TEV-PH1, contained the entire coding region of P4H1 with the following sequence appended upstream of the N-terminal Met of P4H1: MGSSHHHHHHSSGRENLYFQGH.

E. coli strains BL21(DE3) pLysS and BL21-Gold(DE3) were transformed with pET15TEV-PH1 and induced as described above. Frozen cell pellets resuspended in *E. coli* lysis buffer was subjected to sonication on ice using a Sonic Dismembranator 550 (Fisher) with a conical microtip (four sets of 30 repetitions of 1 s on and 3 s off). The lysate was supplemented with 5 mM $MgCl_2$, 50 μg/ml RNase A, and 10 μg/ml DNase I; incubated on ice for 15 min; and centrifuged at 16,000 × *g* for 30 min at 4 °C. The soluble fraction (S16) and the pellet (P16), resuspended in lysis buffer, were frozen at −80 °C. Western blot analysis showed that, although larger amounts of His_6-rP4H were present in the P16 fractions than in the S16 fractions of both strains, substantial levels of soluble protein were also found (data not shown).

For purification, the S16 fraction from a transfected BL21-Gold(DE3) clone expressing high levels of His_6-P4H1 based on Western blot analysis (see below) was brought to 5 mM dithiothreitol, 0.5 M NaCl, and 5 mM imidazole (high purity; Research Organics, Inc.) and applied to a 1-ml HisTrap HP column (Amersham Biosciences) equilibrated in binding buffer (20 mM Tris-HCl (pH 7.9), 0.5 M NaCl, 5 mM dithiothreitol, and 5 mM imidazole). The column was washed with 4 column volumes of binding buffer and 5 volumes of wash buffer (20 mM Tris-HCl (pH 7.9), 0.5 M NaCl, 5 mM dithiothreitol, and 60 mM imidazole). The column was eluted stepwise with 1.2 volumes each of 125 mM, 250 mM, 500 mM, and 1 M imidazole in binding buffer.

Protein Determination—Total protein concentrations were determined using a Coomassie Blue dye binding assay (Pierce). Skp1 and P4H1 protein concentrations were estimated by comparison of the Coomassie Blue-stained bands after SDS-PAGE with the intensity of similar levels of known amounts of molecular weight standards (Dalton Mark VII-L, Sigma).

SDS-PAGE and Western Blotting—Samples were diluted in concentrated SDS sample buffer at a final concentration of 5 mM dithiothreitol; heated in boiling water for 3 min; and applied to a 7–20, 15–20, 12, or 15% polyacrylamide gel as indicated. Proteins were transferred to a 0.45-μm pore diameter nitrocellulose membrane using a Bio-Rad semi-dry blotting apparatus as described (37). Blots were probed for His-tagged proteins using a 1:2000 dilution of anti-His antigen (Novagen) in a 1:1 dilution of blocking buffer (Li-Cor Biosciences) with 0.1% Tween 20 in 150 mM NaCl and 20 mM sodium phosphate (pH 7.4), followed by Alexa Fluor 680-conjugated goat anti-mouse IgG (Li-Cor Biosciences) diluted 1:10000 in diluted blocking buffer, and imaged at 700 nm in a Li-Cor Biosciences Odyssey infrared scanner. Apparent molecular weight values were estimated using the Benchmark prestained protein ladder from Invitrogen.

RESULTS

Detection and Partial Purification of Skp1 P4H Activity—To search for Skp1 P4H activity in the cytosol of *Dictyostelium*, assay conditions were adapted from studies on collagen-type and HIFα-type P4Hs (26, 27, 38). Cosubstrates and cofactors predicted to be important for this class of enzymes include O_2 (derived from the ambient environment), α-ketoglutarate, ascorbate, and Fe^{2+} (added as described under "Experimental Procedures"). The acceptor substrate was unhydroxylated rSkp1A expressed in and purified from *E. coli*. Accumulation of the predicted reaction product, Skp1 hydroxylated at Pro^{143}, was measured using a second enzymatic reaction that specifically modifies the Hyp residue with GlcNAc. GnT1, the polypeptide α-GlcNAc-transferase that normally modifies Skp1 hydroxylated at Pro^{143}, was expressed in *E. coli* as rGnT1, partially purified, and added with UDP-[^{3}H]GlcNAc after 2 h of incubation, and the reaction was continued for 2 h. rGnT1 was not inhibited by the P4H cosubstrates and cofactors in control experiments using Skp1A1-Myc (isolated from strain HW120) purified from *Dictyostelium* as the acceptor substrate (data not shown). As shown in Fig. 1, addition of a soluble S100 extract from stationary phase *Dictyostelium* cells stimulated substantial incorporation of radiolabel into the Skp1 band using the SDS-PAGE assay. Negligible incorporation was observed at zero time if EDTA was added or when rSkp1 or α-ketoglutarate, ascorbate, and Fe^{2+} were not provided. Incorporation was blocked even when $MgCl_2$ was added at 10 mM in the second step (because EDTA also inhibits GnT1). A lower level of incorporation was observed in the absence of added rGnT1, consistent with the presence of endogenous GnT1 in this extract (15).

To further characterize the activity of P4H, the S100 fraction was passed over a DEAE-Sepharose anion exchange column.

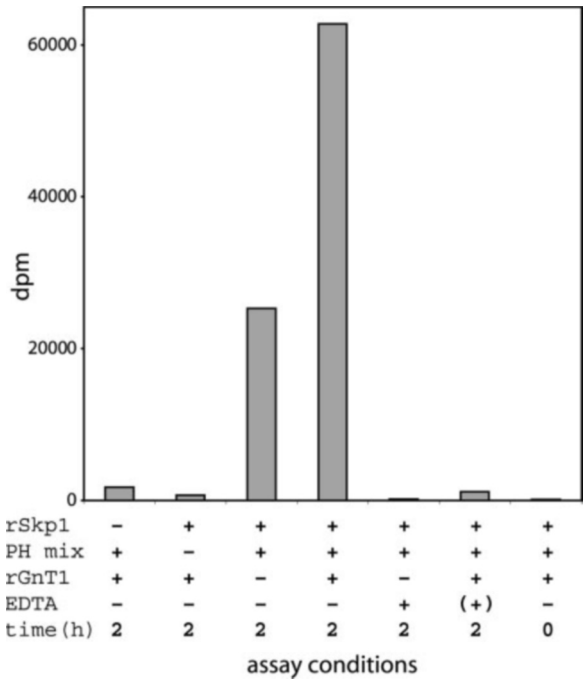


FIG. 1. **Detection of Skp1 P4H activity in a cytosolic extract from *Dictyostelium*.** A cytosolic fraction (S100) was isolated from stationary phase cells, desalted by gel filtration, and tested for Skp1 P4H activity using the two-step coupled P4H assay (see "Experimental Procedures") for 0 or 2 h during the second step as indicated. Activity was measured as GnT1-mediated transfer, during the second step, of ^{3}H from UDP-[^{3}H]GlcNAc into Skp1 using the SDS-PAGE assay. Individual reactions were deprived, as indicated, of added His_{10}-rSkp1A, P4H cofactors and cosubstrates (*PH mix*; α-ketoglutarate, ascorbate, and Fe^{2+}), or rGnT1. As indicated, 5 mM EDTA was added to deplete Fe^{2+}, but because EDTA inhibited GnT1 activity, $MgCl_2$ was added at 10 mM during the second step in the trial indicated *((+))*. The results shown are representative of findings from two independent experiments.

Activity was found to co-elute in a retarded flow-through fraction in good yield (data not shown), as observed previously for GnT1 (15). This large pool was brought to 20% $(NH_4)_2SO_4$ and loaded onto a phenyl-Sepharose column, on which it was retained. The column was eluted with a descending gradient of $(NH_4)_2SO_4$ and then an ascending gradient of ethylene glycol. Skp1 P4H activity eluted in the ethylene glycol gradient in a single peak that preceded but partially overlapped with that of GnT1, with a yield of 10% (data not shown). Although the Skp1 P4H activity behaved as a single entity and was partially active after separation from the bulk of the cellular proteins, the activity loss suggested that a biochemical approach to characterizing P4H would be problematic. An alternative approach was taken to identify the Skp1 P4H gene.

Cloning the Candidate Dictyostelium Skp1 P4H Gene—Genomic analysis identified five potential P4H genes, and each is predicted to encode a cytoplasmic protein (12). As summarized in the Introduction, one of these, *phyA*, is the best candidate for encoding Skp1 P4H based on a comparative bioinformatics approach. *phyA* is present as a single copy on chromosome 2 (25). The primary model for the *phyA* coding region (described by dictyBaseID DDB0169393) consists of 1068 nucleotides, including two introns (nucleotides 283–378 and 626–744). The predicted start codon of *phyA* lies 272 nucleotides downstream of the beginning of a predicted reverse-oriented two-exon gene defined by four expressed sequence tags (*e.g.* dictyBaseID DDB0019707). There are no plausible additional exons in this region, in support of the computer-generated model. The ATG start codon is preceded at position −3 by T, which is found less frequently than A, but is compatible with the expression of a transgene in *Dictyostelium* (39). The predicted *phyA* stop codon (TAA) is separated by 100 nucleotides from the stop codon of the downstream reverse-oriented gene likely to be the ortholog of the yeast glycosyltransferase *alg10* (40). This region is very A/T-rich, with a poly(A) stretch, putative polyadenylation signals (AATAAA) in both directions, and multiple nucleotide repeats and therefore appears to represent a true intergenic region.

The existence of *phyA* in strain Ax3 was confirmed by amplification of genomic DNA using primers PHF-S and PHF-AS (Fig. 2), which yielded a 1.1-kb DNA fragment with a nucleotide sequence (Fig. 2) that exactly matches that of dictyBaseID DDB0169393. The predicted protein coding region of *phyA* was prepared by reverse transcription-PCR using total cell RNA and the same two primers as described above as described under "Experimental Procedures." This yielded an 850-bp DNA fragment, whose sequence confirmed that the primer sequences, which represent the expected N and C termini, were present in the processed transcript and verified the positions of the two predicted introns, as shown in Figs. 2 and 3*A*. The three exons comprise 852 nucleotides encoding a potential polypeptide of 284 amino acids with an M_r of 33,348 and a predicted pI of 6.9. This sequence is not represented in the Tsukuba Expressed Sequence Tag Library (available at dictycdb.biol.tsukuba.ac.jp/), suggesting that its mRNA is not abundant.

The second amino acid after the initial Met is Asp, predicted to be a secondary destabilizing residue according to the N-end rule for yeast and mice (41). EGL9, an HIFα-type P4H from *Caenorhabditis elegans*, is also initiated by this sequence. The predicted protein sequence lacks a hydrophobic cluster that might target it to membranes and lacks basic motifs found in some nuclear targeting signals. As described previously (12), the coding region includes two homology domains (Fig. 3*B*) characteristic of HIFα-type P4Hs in animals. The inferred catalytic domain region (*CD*) contains the conserved triad of conserved Fe^{2+}-coordinating residues (see the Introduction and Fig. 2), and its conserved α-ketoglutarate-coordinating basic residue (Fig. 2) is spaced from the upstream conserved His residue like that of P4Hs rather than certain other α-ketoglutarate-dependent dioxygenases. The basic residue is Arg rather than Lys, which is found in collagen-type P4Hs. Overall, the sequence of P4H1 is more similar to HIFα-type P4Hs than to collagen-type P4Hs or prolyl 3-hydroxylases found in the rough endoplasmic reticulum. For example, within the more conserved 120-amino acid catalytic domain region, P4H1 is 33% identical and 52% similar to human HPH1 (HIFα-type), but only 17% identical and 41% similar to human collagen type I P4H and 19% identical and 40% similar to human prolyl 3-hydroxylase-1 (42). Relative to known HIFα-type P4Hs, P4H1 appears to be close to the minimal protein length defined by human HPH1 (239 amino acids).

Overexpression of phyA in Dictyostelium—To test for Skp1 P4H activity, the *phyA* cDNA was inserted into the previously described *Dictyostelium* expression vector pVS so that the expressed full-length protein would bear a C-terminal c-Myc epitope tag (Fig. 3*C*). pVS is an integrating plasmid that confers resistance to G418 and that directs constitutive expression during growth and early development under control of the discoidin-1γ promoter. Drug-resistant primary cultures (prior to cloning) were lysed, fractionated by differential centrifugation into insoluble P100 and soluble S100 fractions, and analyzed for expression of a novel protein reactive with mAb 9E10, which detects the Myc epitope, by Western blot analysis. The S100 fraction contained a novel mAb 9E10-reactive band with an apparent M_r of 30,000 (Fig. 4*A*), similar to the expected M_r of 34,500 (including the Myc tag). This band, referred to as

```
1    M  D  I  S  N  L  P  P  H  I  R  Q  Q  I  L  G  L  I  S  K
1    ATGGATATTTCTAACTTACCCCCTCACATAAGACAACAAATATTAGGTTTAATTAGTAAA  PHF-S

21   P  Q  Q  N  N  D  E  S  S  S  S  N  N  K  N  N  L  I  N  N
61   CCACAACAAAATAATGATGAAAGTAGTAGCAGTAACAACAAAAACAATTTAATAAATAAT

41   E  K  V  S  N  V  L  I  D  L  T  S  N  L  K  I  E  N  F  K
121  GAAAAAGTTTCAAATGTTCTAATTGATTTAACCAGTAATTTAAAAATAGAAAATTTTAAA

61   I  F  N  K  E  S  L  N  Q  L  E  K  K  G  Y  L  I  I  D  N
181  ATCTTCAACAAAGAATCATTAAATCAATTAGAAAAAAAAAGGTTATTTAATAATTGATAAT

81   F  L  N  D  L  N  K  I  N  L  I  Y  D  E
241  TTTTTAAATGATTTAAATAAAATAAATTTAATTTATGATGAAgtaagtggaaaaaaaaaa

301  aaataaaaataaattaggttttaattcttttttttttttttttttttttttttttttt

95                    S  Y  N  Q  F  K  E  N  K  L  I  E  A  G
361  atttttggtaaaataaagTCATACAATCAATTTAAAGAAAATAAATTAATAGAAGCAGG

109   M  N  K  G  T  D  K  W  K  D  K  S  I  R  G  D  Y  I  Q  W
421  TATGAACAAAGGTACAGATAAATGGAAAGATAAATCAATTAGAGGTGATTATATTCAATG

129   I  H  R  D  S  N  S  R  I  Q  D  K  D  L  S  S  T  I  R  N
481  GATACATAGAGATTCAAATAGTAGAATTCAAGATAAAGATTTATCATCAACAA***TTCGAA***A  BstBI

149   I  N  Y  L  L  D  K  L  D  L  I  K  N  E  F  D  N  V  I  P
541  TATTAATTATTTATTAGATAAATTAGATTTAATAAAAAATGAATTTGATAATGTTATACC

169   N  F  N  S  I  K  T  Q
601  AAATTTTAATTCAATTAAAACTCAAgtatgtttttttttttttttaatttcattttattt

661  ttattattaaattttcaaaaatgttaacatttgtatttttttattatttgtatataaaaaa

177                           T  Q  L  A  V  Y  L  N  G  G  R  Y
721  aaaaattaaaaaaaaaaaaaaaaagACACAATTAGCAGTTTATTTAAATGGTGGTAGATAT

189  I  K  H  R  D  S  F  Y  S  S  E  S  L  T  I  S  R  R  I  T
781  ATTAAACATAGAGATTCATTTTATTCCTCAGAATCATTAACAATATCAAGAAGAATTACA

209  M  I  Y  Y  V  N  K  D  W  K  K  G  D  G  G  E  L  R  L  Y
841  ATGATTTATTATGTTAATAAAGATTGGAAGAAAGGTGATGGTGGAGAATTAAGATTATAT

229  T  N  N  P  N  N  T  N  Q  K  E  L  K  Q  T  E  E  F  I  D
901  ACTAATAATCCAAATAATACAAATCAAAAAGAATTAAAACAGACTGAAGAATTTATAGAT

249  I  E  P  I  A  D  R  L  L  I  F  L  S  P  F  L  E  H  E  V
961  ATTGAACCAATAGCTGATAGATTATTAATATTTTTAAGTCCATTTTTAGAACATGAAGTT

269  L  Q  C  N  F  E  P  R  I  A  I  T  T  W  I  Y  *
1021 TTACAATGTAATTTTGAACCAAGAATTGCAATTACAACTTGGATTTATtaa          PHF-AS
```

FIG. 2. **P4H1 sequence.** *phyA* is a predicted gene from the *Dictyostelium* Genome Sequencing Project (GenBank™/EBI accession number AC115612.2) and dictyBase (dictyBaseID DDB0169393). The nucleotide sequence shown derives from PCR amplification of *Dictyostelium* strain Ax3 genomic DNA using primers PHF-S and PHF-AS (*underlined*). Exons were determined using the same two primers in reverse transcription-PCR amplification of total cell RNA. Key *phyA* amino acids are shown in *boldface* and *underlined*, and the BstBI site used for inserting the *bsr* cassette is in *boldface italics*. This sequence was deposited in the GenBank™/EBI Data Bank under accession number AY768817.

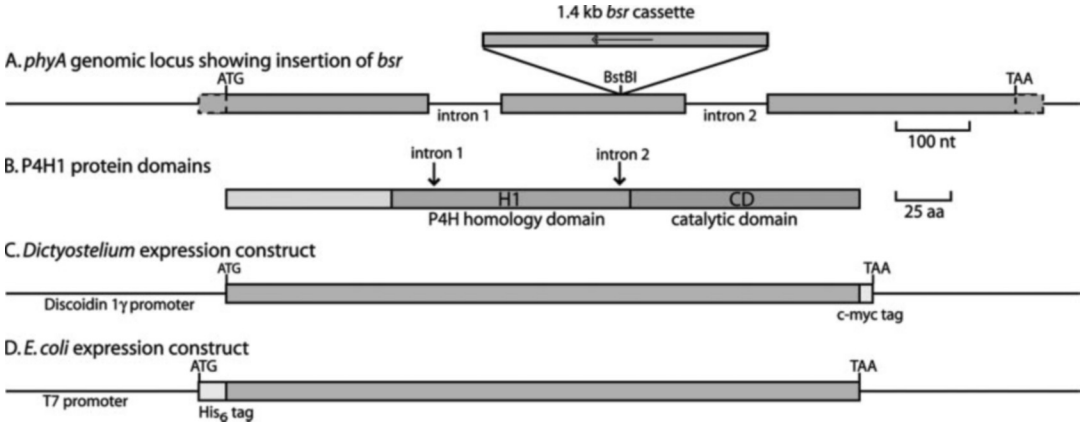


FIG. 3. **Schematic diagram of the *phyA* locus, disruption strategy, and expression constructs.** *A*, genomic locus of *phyA* illustrating the intron-exon organization and deduced amino acid (*aa*) coding region. Insertion of the *bsr* cassette in the BstBI site is illustrated. *nt*, nucleotides. *B*, the predicted encoded protein P4H1, showing the inferred P4H H1 homology domain (12) and the catalytic domain (*CD*) (47) and positions of introns. *C*, diagram of the *Dictyostelium* expression construct in pVS, depicting the c-Myc tag at the C terminus of the full-length coding region. *D*, diagram of the *E. coli* P4H1 expression construct in pET15TEVi, showing the His_6 tag at the N terminus of the full-length coding region.

P4H1-Myc, was not detectable in the P100 fraction, suggesting that P4H1 is a soluble cytoplasmic protein, consistent with the absence of apparent organelle targeting motifs. Other mAb 9E10-reactive bands were present in the control cells and are not related to P4H1. Clones from primary cultures grown in 120 or 20 μg/ml G418 for multiple passages expressed distinct

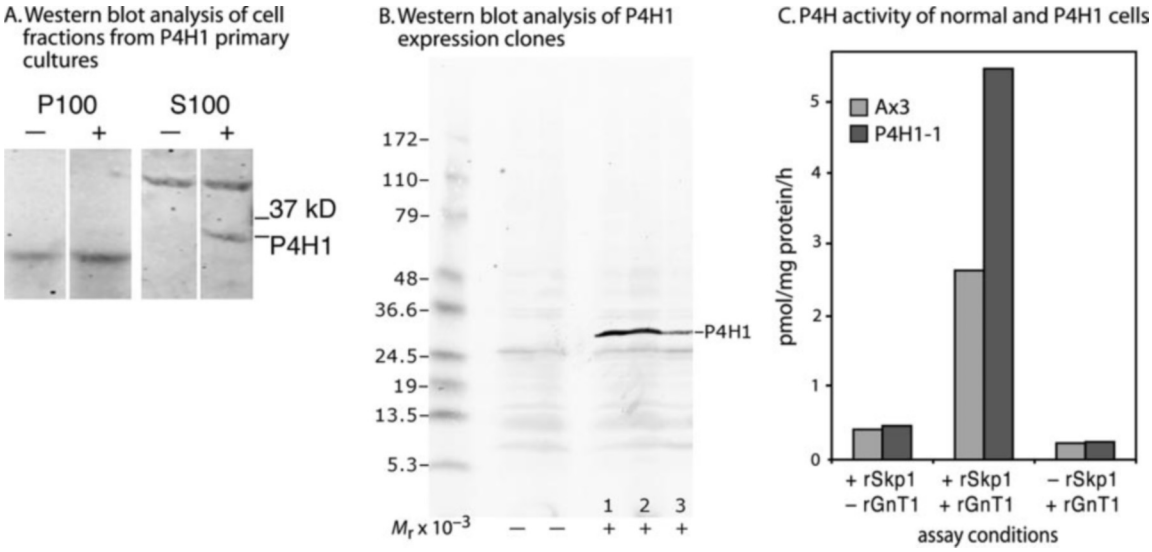


FIG. 4. **Overexpression of *phyA* in *Dictyostelium*.** *A*, the expression construct described in the legend to Fig. 3*C* was electroporated into *Dictyostelium*. Primary drug-resistant cells (prior to cloning) transfected with pVS (empty vector; −) or pVS-P4H1 (+) were gently lysed and fractionated by ultracentrifugation at 100,000 × *g* for 60 min to yield a soluble cytoplasmic extract (S100) and a particulate fraction (P100). Extracts were subjected to SDS-PAGE and Western blot analysis using mAb 9E10 to detect the c-Myc epitope tag. A novel band at M_r 30,000 was seen only in the S100 fraction of pVS-P4H1-transfected cells. *B*, soluble S100 extracts were from rP4H1-Myc expression clones (strains HW285–287; labeled *1–3*; +) and control pVS-transfected clones (−) harvested at stationary phase. *C*, S100 extracts of the high level expresser clone 1 from *B* and Ax3 (parental) cells were desalted and assayed for Skp1 P4H activity using the standard one-step/SDS-PAGE assay (see "Experimental Procedures") in the presence of added His_{10}-rSkp1A and/or rGnT1 as indicated. The results shown are representative of two independent experiments.

levels of P4H1-Myc (Fig. 4*B*), with high level expressers enriched in the primary cultures passaged at the higher compared with the lower G418 concentration (data not shown).

A soluble S100 extract of clone 1, which expressed a high level of P4H1-Myc, was compared with an extract from the parental strain (Ax3) for Skp1 P4H activity (Fig. 4*C*). In the presence of added His_{10}-rSkp1A and rGnT1, clone 1 extracts were found to have >2-fold higher specific Skp1 P4H activity compared with Ax3 extracts. No difference between parental Ax3 and clone 1 cells was observed in the absence of added rSkp1 and rGnT1, indicating that these two proteins are rate-limiting under these conditions. These results suggest that *phyA* encodes a soluble cytoplasmic protein with Skp1 P4H activity and that the C-terminal Myc tag does not block activity.

Expression of phyA in E. coli—To confirm the activity of P4H1 suggested by transfection of *Dictyostelium*, *phyA* was expressed in a heterologous system. The full-length cDNA for the *phyA* coding region was inserted into pET15TEVi, an isopropyl 1-thio-β-D-galactopyranoside-inducible *E. coli* expression vector designed to produce the native protein with an N-terminal His_6 tag (Fig. 3*D*). Several clonal isolates yielded soluble extracts containing P4H1 protein that could be detected using anti-His_6 antibody at the same molecular weight position as P4H1-Myc expressed in *Dictyostelium* (data not shown). These extracts also showed substantial Skp1 P4H activity using the assay used for *Dictyostelium* extracts, and non-transfected extracts showed <10% incorporation (data not shown).

His_6-rP4H1 was purified from S100 extracts of *E. coli* by passage over an Ni^{2+} column as described under "Experimental Procedures." This one-step purification produced a highly purified preparation of P4H1 based on Coomassie Blue staining of an SDS-polyacrylamide gel (Fig. 5*A*) and Western blot analysis using anti-His_6 antibody (Fig. 5*B*). The major band visible upon Coomassie Blue staining appeared to be reactive with anti-His_6 antibody. Chromatography was performed in the absence of the predicted cosubstrates and cofactors to assess their roles in subsequent add-back experiments.

Characterization of rP4H1—In preliminary trials, highly purified His_6-rP4H1 exhibited Skp1 P4H activity in the one-step coupled assay using SDS-PAGE analysis to confirm incorporation into Skp1. Activity was linear with respect to time and proportional to enzyme amount (data not shown). To quantitate activity, the amount of rGnT1 was adjusted so that, at the highest concentrations of His_6-rP4H1 and His_{10}-rSkp1A tested, initial velocity was within 90% of the measurable maximum. The concentrations of the predicted P4H1 cosubstrates and cofactors were within 50% of the optimal values (except for O_2) based on the results shown below. Under these conditions, Skp1 P4H activity was hyperbolically dependent on His_{10}-rSkp1A, yielding an apparent K_m of 0.2 μM (Fig. 6*A*). Assuming

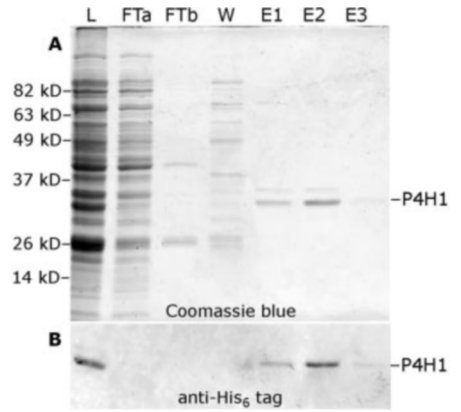


FIG. 5. **Expression of P4H1 in *E. coli*.** A soluble S16 extract from an *E. coli* clone expressing P4H1 (Fig. 3*D*) was applied to and eluted from an Ni^{2+}-Sepharose column. *A*, samples were analyzed on a 12% SDS-polyacrylamide gel and stained with Coomassie Blue. Positions of molecular mass markers are shown on the left. *B*, a parallel gel was analyzed by Western blotting using anti-His_6 antibody and a fluorescent secondary antibody. *L*, crude S16 extract; *FTa* and *FTb*, flow-through fractions; *W*, wash fraction containing 60 mM imidazole and 500 mM NaCl; *E1*, elution fraction containing 125 mM imidazole in 500 mM NaCl; *E2*, elution fraction containing 250 mM imidazole in 500 mM NaCl; *E3*, elution fraction containing 500 mM imidazole in 500 mM NaCl.

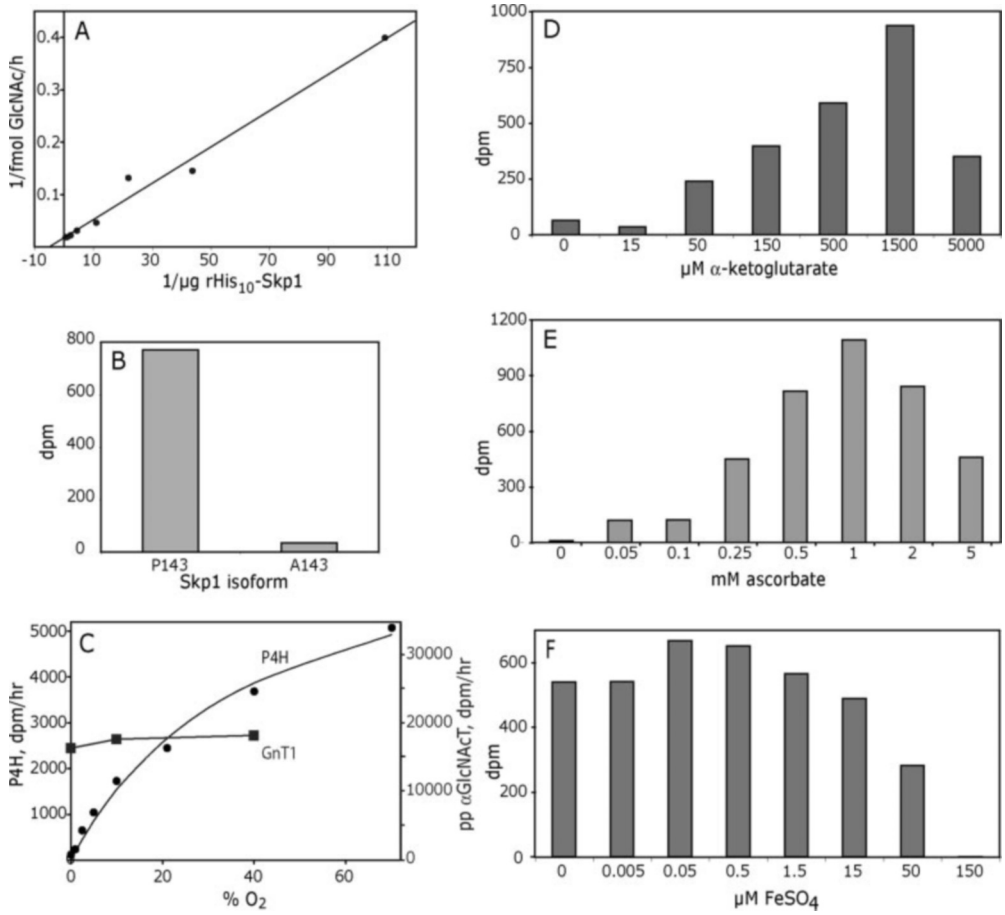


FIG. 6. **Characterization of rP4H1 enzyme activity.** The activity of purified His_6-rP4H1 (fraction *E2* in Fig. 5) was assayed using the standard one-step coupled assay except as indicated. *A*, dependence on concentration of His_{10}-rSkp1A. Shown is a double-reciprocal plot of the data. Apparent K_m and V_{max} values were calculated based on the line, which represents the least-squares best fit of the data. *B*, acceptor activity of equal concentrations of His_{10}-rSkp1A and rSkp1A(P143A). *C*, dependence on O_2 concentration. The curve shows the best hyperbolic fit of the data, which was used to calculate the apparent K_m. This panel also shows the dependence of rGnT1 (*pp αGlcNAcT*) activity on O_2 using Skp1A1-Myc as the acceptor. *D*, dependence on α-ketoglutarate concentration. *E*, dependence on ascorbic acid concentration. *F*, dependence on added Fe^{2+} concentration. The results shown are representative of results from two independent sets of experiments.

that hydroxylated Skp1 is modified by [^{3}H]GlcNAc in the coupled assay before it saturates GnT1, which has an apparent K_m of 0.6 μM measured using mutant Skp1A1-Myc (15), this result suggests that the two enzymes have a similar high affinity for their targets. Subsequent reactions contained 0.9 μM rSkp1. The V_{max} from this experiment was estimated at 6 nmol of GlcNAc/μmol of enzyme protein/min. Even after correction for suboptimal levels of α-ketoglutarate and O_2 (see below), the value was 60 nmol/μmol/min. Although higher than the 7 nmol/μmol/min (43) and 0.5 nmol/μmol/min (44) values reported for purified human recombinant HIFα P4Hs using optimized peptide substrates, it is far lower than the specific activities reported for recombinant or native P4Hs in crude extracts (27, 43). At present, it is not known if the low specific activity is a property of the enzyme preparation or the target substrate (see "Discussion"). In either case, use of highly purified enzyme and substrate suggests that the action of P4H1 on Skp1 is direct.

Hydroxylation of Skp1 in this reaction is expected to occur at Pro^{143} based on the specificity of the GnT1-based reaction employed to assay the hydroxylation event. To confirm this, a mutant form of Skp1 in which Pro^{143} was replaced with Ala was expressed in and purified from *E. coli* as described under "Experimental Procedures." Mutant rSkp1A(P143A) was inactive as an acceptor substrate (Fig. 6*B*), indicating that Pro^{143} is required for and is probably the target for P4H1-mediated hydroxylation, as occurs *in vivo* (16).

The predicted cosubstrate α-ketoglutarate was required for activity, and the optimal concentration was found to be 1.5 mM (Fig. 6*D*). Higher concentrations were inhibitory, but the mechanism of this effect is unknown. Under the conditions of the assay, dependence on this substrate did not follow simple Michaelis-Menten kinetics, but the projected K_m of P4H1 for this substrate appears to be substantially higher than the values of 55–60 μM (27) and 3–5 μM (44) reported for human HIFα P4Hs. Ascorbate, required by other known P4Hs, was also needed by P4H1 (Fig. 6*E*). The optimal concentration was 1 mM, and higher concentrations were inhibitory. P4H1 appears to have a lower affinity for ascorbate compared with human HIFα P4Hs, whose ascorbate K_m values range from 140 to 170 μM (27, 44). Addition of Fe^{2+} in the form of $FeSO_4$ did not stimulate activity (Fig. 6*F*). Because Fe^{2+} is required for this class of enzymes (20, 21, 24), it is likely that this ion is tightly bound, as observed for human HIFα-type P4Hs (19, 38). The concentrations of compounds tested in these experiments did not inhibit rGnT1 activity (tested using Skp1A1-Myc) by >10% (data not shown). Finally, the enzyme was dependent on O_2 (Fig. 6*C*). The enzyme was not saturated at atmospheric O_2 (21% or 250 μM), and a double-reciprocal plot of the data yielded a straight line describing an apparent K_m of 40% or 480 μM O_2. This compares with K_m values of 230–250 μM for human HIFα P4Hs (27, 45). rGnT1 activity was not affected over this O_2 concentration range (Fig. 6*C*).

Inhibitors of P4H1—Skp1 glycosylation was previously observed to be inhibited by treatment of cells with two known

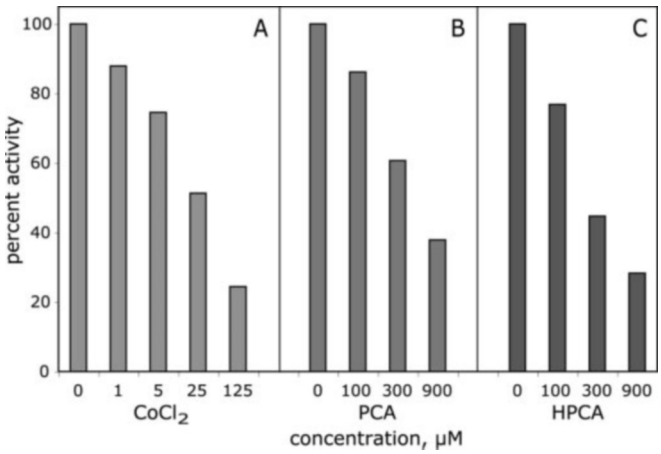


FIG. 7. **Inhibition of rP4H1 activity.** Activity was determined using the standard one-step assay. *A*, activity in the presence of increasing concentrations of $CoCl_2$. *B*, activity in the presence of increasing concentrations of 3,4-dihydroxybenzoate (*PCA*). *C*, activity in the presence of increasing concentrations of 3,4-dihydroxyphenyl acetate (*HPCA*). The highest concentrations of inhibitors tested did not inhibit GnT1 by >11% (data not shown). The results shown are averaged from two independent trials.

inhibitors of P4Hs, α,α′-dipyridyl and the ethyl ester of 3,4-dihydroxybenzoate (16). Highly purified His_6-rP4H1 was inhibited *in vitro* by 3,4-dihydroxybenzoate in a concentration-dependent manner (Fig. 7*B*). 3,4-Dihydroxyphenyl acetate inhibited P4H1 similarly (Fig. 7*C*). 50% inhibition occurred only at ≥300 μM, which is more similar to the weak effects of these compounds on HIFα-type P4Hs than to their strong effects on collagen-type P4Hs (27). α,α′-Dipyridyl inhibited GnT1, so its effect on P4H1 could not be tested. Another inhibitor of animal HIFα-type P4Hs, $CoCl_2$ (19, 44, 46), inhibited His_6-rP4H1, with a half-maximal effect at ~25 μM (Fig. 7*A*). $CoCl_2$ might compete with binding of Fe^{2+} to the enzyme. $ZnCl_2$ was not tested because it inhibited rGnT1 (data not shown). Desferrioxamine (deferoxamine), thought to function as an Fe^{2+} chelator, exerted only weak, 30% inhibition at 310 μM, in contrast to the more potent effects on HIFα-type P4Hs (19, 46). These compounds did not inhibit GnT1 by >11% at the highest concentrations tested (data not shown), showing that their effects were specific for P4H1 in the coupled assay.

Disruption of the Dictyostelium phyA Gene—To determine whether P4H1 is required for Skp1 hydroxylation *in vivo*, the effect of disrupting the *phyA* gene was examined. The genomic fragment of *phyA* was modified by addition of a *bsr* cassette to the unique BstBI site (as shown in Fig. 3*A*), excised from the parental plasmid, and trimmed with Bal-31 exonuclease to remove terminal non-homologous sequences. To induce gene disruption by homologous recombination, the modified *phyA* DNA fragment was electroporated into *Dictyostelium* cells. Blasticidin-resistant cells grew at high frequency. Screening of drug-resistant clones by PCR yielded clones whose *phyA* gene length (2.5 kb) was either increased by the size of the *bsr* cassette, suggesting occurrence of the desired homologous recombination, or not affected (1 kb), suggesting insertion elsewhere in the genome (Fig. 8*A*). Two clonal isolates that amplified the longer PCR product, one that amplified the shorter product (*bsr*), and one from a parental clone (Ax3) were extracted and analyzed for Skp1 P4H activity (Fig. 8*B*). Extracts from cells whose *phyA* locus was altered (clones 1a and 1b) exhibited negligible activity, in contrast to extracts from the parental strain (Ax3) or from the drug-resistant clone whose *phyA* was not altered (*bsr*). Absence of P4H activity in the mutant extracts could be complemented biochemically by addition of purified His_6-rP4H1, confirming the specificity of the

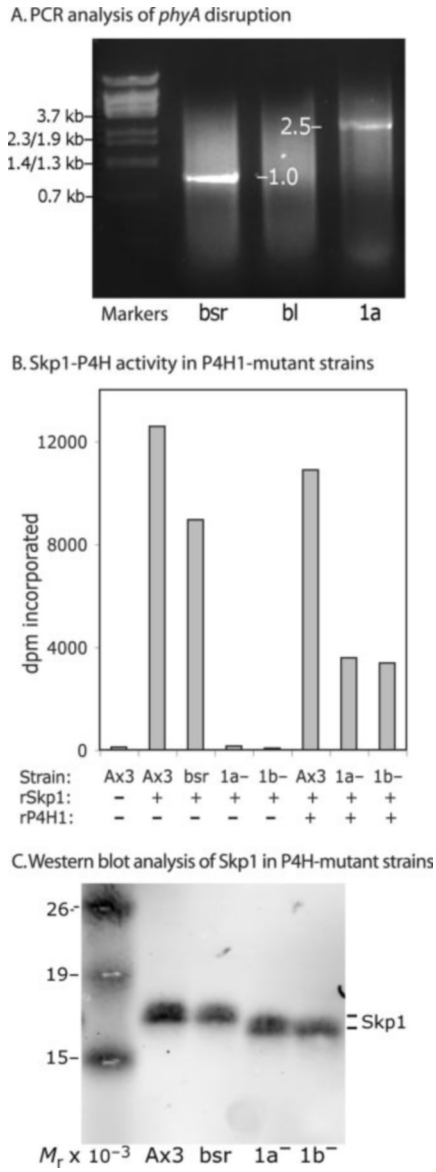


FIG. 8. **Disruption of the *Dictyostelium phyA* locus.** A nearly full-length fragment of the *phyA* (P4H1) coding region was modified by insertion of a *bsr* cassette (as illustrated in Fig. 3*A*), trimmed with Bal-31 exonuclease, and electroporated into *Dictyostelium* strain Ax3 cells. *A*, blasticidin-resistant cell clones were analyzed for modification of the *phyA* locus using PCR. Strain HW288 (clone 1a) and a control strain (*bsr* inserted into an unknown location) are shown after amplification of genomic DNA using primers PHF-S and PHF-AS (Fig. 2). The results from a control reaction containing irrelevant primers are also shown (*bl*). Molecular size markers are shown in the *first lane*. *B*, S100 extracts of strain HW288 (clone 1a), strain HW289 (clone 1b), the parental strain (Ax3), and the bsr^+ control strain were assayed for Skp1 P4H activity using the standard one-step assay. Reactions were supplemented with purified His_{10}-rSkp1A and/or purified His_6-rP4H1 as indicated. *C*, the apparent M_r of Skp1 from mutant clones 1a and 1b (10^6 whole cells/lane) was compared with that of normal Skp1 from the parental (Ax3) and bsr^+ control strains by Western blot analysis using mAb 4E1 after separation on a 15–20% SDS-polyacrylamide gel. The anomalous migration of Skp1 between the M_r 19,000 and 15,000 markers is unique to the prestained molecular weight markers employed in this experiment. The results shown are representative of results from two independent experiments.

mutation. To determine whether hydroxylation of Skp1 was affected, cell extracts were analyzed by SDS-PAGE and Western blotting to compare the apparent molecular weight of the Skp1 proteins. The apparent molecular weight of Skp1 was decreased in the two clones lacking P4H activity (Fig. 8*C*), as expected from the absence of hydroxylation-dependent glycosy-

lation, relative to the control strains. As a result of disruption of the *phyA* locus, cell extracts lacked measurable P4H activity and expressed Skp1 with a smaller apparent molecular weight, indicating that P4H1 is the Skp1 P4H *in vivo*. *phyA* mutant cells proliferated in HL-5 medium at the same rate as parental cells (data not shown).

DISCUSSION

Hydroxylation of *Dictyostelium* Skp1 appears to be directly mediated by P4H1, the product of the *phyA* gene. The P4H1 protein has the intrinsic ability, when expressed recombinantly in and purified from *E. coli* (Fig. 5), to modify rSkp1A, also expressed in and purified from *E. coli*, in such a way that it then becomes a substrate for GnT1 (Fig. 6*A*), the polypeptide α-GlcNAc-transferase that initiates subsequent glycosylation of Skp1. Modification depends on the presence of Pro^{143} in Skp1, the site of *in vivo* hydroxylation, as the Skp1(P143A) mutant was not modified (Fig. 6*B*). Furthermore, overexpression of *phyA* in *Dictyostelium* led to higher Skp1 P4H activity in extracts (Fig. 4*C*), although this did not alter the (small) fraction of Skp1 that was not hydroxylated, which therefore appears to be controlled by other factors. Finally, disruption of *phyA* by homologous recombination-mediated insertion of a *bsr* cassette into the middle of the coding region abolished detectable Skp1 P4H activity in extracts (Fig. 8*B*) and resulted in the expression of a lower molecular weight form of Skp1 (Fig. 8*C*), consistent with the absence of hydroxylation-dependent glycosylation. The other four putative P4H genes (12) do not substitute for the missing P4H1 to hydroxylate Skp1.

His_6-rP4H1 exhibited a high affinity for His_{10}-rSkp1A, with an apparent K_m of 0.2 μM, which is slightly lower than the submicromolar K_m for the subsequently acting GlcNAc-transferase, GnT1 (15). This value is an order of magnitude lower than that of HIFα P4Hs measured using synthetic peptides derived from different HIFαs (27). The difference may be due to the use of the full-length acceptor protein for P4H1. Little or no activity[2] was observed using a 22-mer synthetic peptide from Skp1 (15), but this can be attributed to the poor activity of GnT1 for the hydroxylated peptide. However, in its highly purified state, the enzyme exhibited a V_{max} of only 60 nmol of GlcNAc/μmol of P4H1/min. Although higher than values reported for purified recombinant HIFα P4Hs (43, 44), it is $\sim$0.1% of the values inferred for human HIFα P4Hs in cytosolic extracts (27, 45). Similarly, P4H1-Myc expressed in *Dictyostelium* cells appears to have a higher specific activity. A calculation based on activity in Fig. 4*C* relative to an upper limit estimate of P4H1 in Fig. 4*B* of 0.1 μg/lane yields a conservative estimate for activity of $\geq$2 μmol/μmol/min. Therefore, optimal activity may require *Dictyostelium* factors, which is consistent with the loss of activity observed during purification of Skp1 P4H from extracts. Further studies are required to determine whether the low V_{max} is a property of the enzyme or the acceptor substrate. His_6-rP4H1 might be affected by its N-terminal His_6 tag or be unstable, as suggested by 3-fold losses encountered during freeze-thaw cycles (data not shown). The N-terminal His tag of His_{10}-rSkp1A may affect its substrate activity, as point mutations in the N-terminal domain of Skp1A1-Myc result in the accumulation of unhydroxylated isoforms *in vivo* (7). Alternatively, Skp1, normally present in heteromeric protein complexes (see the Introduction), may be an inefficient substrate outside of these complexes. Very low activity was also described for GnT1 using the same Skp1A1-Myc mutant as an acceptor (15).

P4H1 is similar to the HIFα class of P4Hs that has been described in vertebrate and invertebrate animals (20, 21, 24). P4H1 is the most related in sequence of the five *Dictyostelium* P4H genes predicted from genomic sequence analysis (12). P4H1 is $\sim$35% identical and 63% similar to the *C. elegans* homolog EGL9 over the H1 and catalytic domains (Fig. 3*B*). A phylogenetic analysis of H1 and catalytic domain sequences from 35 potential P4Hs places P4H1 and predicted proteins from other microorganisms, including a diatom and an oomycete, together in the same subclade with the animal HIFα P4Hs (12). The similarity suggested by sequence analysis is borne out by functional studies. P4H1 is sufficient for catalyzing hydroxylation of Skp1, except for a possible, untested requirement for GnT1. It is a soluble protein (Fig. 4*A*) and appears to reside in the cytoplasm based on differential centrifugation and the absence of basic type nuclear localization sequences. However, P4H1 is small enough to equilibrate in the nucleus, which may be a site of action of some animal HIFα-type P4Hs (48).

Like all P4Hs (20, 21, 24), rP4H1 is critically dependent on the cosubstrates α-ketoglutarate (Fig. 6*D*) and O_2 (Fig. 6*C*) and also requires ascorbate (Fig. 6*E*), which might protect the enzyme from Fe^{2+} oxidation (22). P4H1 is maximally stimulated at higher concentrations of α-ketoglutarate, ascorbate, and O_2 than required for the human HIFα P4Hs (27), which might correlate with metabolic differences between free-living amebas and cells of a multicellular organism. A dependence of P4H1 on Fe^{2+}, observed for all other P4Hs, could not be demonstrated by purifying the enzyme away from free Fe^{2+} (Fig. 6*F*). Similar observations have been made for HIFα-type P4Hs (19, 27, 38), which bind Fe^{2+} more tightly than do the collagen-type P4Hs. A dependence of P4H1 on Fe^{2+} is consistent with the inhibitory effect of the chelator EDTA (Fig. 1) and $CoCl_2$ (Fig. 7*A*), which has been suggested to compete with Fe^{2+} in HIFα P4Hs (19, 44, 46). The Fe^{2+} inhibitors α,α'-dipyridyl and $ZnCl_2$ were not tested due to inhibitory effects on GnT1. Desferrioxamine had only a weak inhibitory effect (30%) at the highest concentration tested (310 μM), in contrast to the potent inhibitory action of this chelator on HIFα P4Hs (19, 46). However, ascorbate, present at a high concentration in these assays, has been reported to interfere with desferrioxamine inhibition (22). Taken together, the results suggest that P4H1 may bind Fe^{2+} even more tightly than do its animal counterparts. Finally, *Dictyostelium* P4H1 was also susceptible to inhibition by high concentrations of 3,4-dihydroxybenzoate and 3,4-dihydroxyphenyl acetate (Fig. 7, *B* and *C*), thought to affect α-ketoglutarate binding. The ethyl ester of 3,4-dihydroxybenzoate also appears to inhibit Skp1 hydroxylation in cells (16). These compounds are better inhibitors of collagen-type P4Hs compared with P4H1 and HIFα P4Hs (27). Therefore, P4H1 is homologous to animal P4Hs and more closely related to the HIFα (rather than the collagen) class. The existence of collagen-type P4Hs in the secretory pathway of fungi (49), a virus (50), algae (51), vascular plants (52), and animals (17) is well known. The identification of *Dictyostelium* P4H1 as an apparent microbial ortholog of the animal HIFα-type P4Hs suggests that this enzyme type also has an ancient evolutionary lineage. A phylogenetic analysis of 35 sequences suggests that the two classes of P4Hs resulted from an ancient gene duplication that predated the separation of Metazoa from the evolutionary tree of life (12), and the existence of related sequences in certain bacteria (12, 53) is consistent with an occurrence of the proposed gene duplication at the time of the appearance of the eukaryotic secretory apparatus.

The first defined target substrate for the animal HIFα-type P4Hs was HIF1α itself and the related proteins HIF2α and HIF3α (18, 19, 46). HIF1α is modified at two positions by HPH1, and these Pro residues share a common sequence context defined as $LXXLA\mathbf{P}X_{3-4}D_{2-3}$ based on sequence align-

[2] H. van der Wel and C. M. West, unpublished data.

ments. This differs from the Skp1 Pro^{143} context of KNDFT-**P**EEEEQIR. However, site-directed mutagenesis studies have shown that HPH1 is tolerant of amino acid substitutions at the conserved positions (54, 55). In addition, a vascular plant P4H can modify both HIF1α and collagen peptides (52), indicating that other factors influence enzyme target specificity. Nevertheless, based on a genomic survey of acceptor peptide motifs defined by the sequence alignments, RNA polymerase II has also been discovered as a human HPH1 target substrate (56). Identification of P4H targets is experimentally challenging because the hydroxylated product is difficult to detect directly. HIFα-type P4H substrates are known by virtue of recognition of the hydroxylated protein by the VHL protein (44, 57), a subunit of the VHL E3 complex that subsequently polyubiquitinates modified proteins in the cell. This indirect method of detection would miss hydroxylation not recognized by the VHL protein.

Skp1 represents a novel target for cytoplasmic P4Hs. Based on the findings in *Dictyostelium*, animal Skp1 is suggested to be a potential target of one or more of the three known animal HIFα-type P4Hs. Recently, a role for an HIFα-type P4H was defined by genetic analysis of cell growth regulation in *Drosophila* ommatidial cells (58) and for hypoxia-induced accumulation of phosphatidic acid in mammalian cells (59). The targets of the enzyme were suggested not to be an HIFα, and the present findings nominate Skp1 as a candidate. Although the absence of Pro^{143} in mammalian Skp1 proteins (except for its presence in several unconfirmed murine and human expressed sequence tags) suggests that mammalian Skp1 is not subject to this modification, another Pro residue (Pro^{128} in *Dictyostelium*) in a related sequence and secondary structure context is conserved at a position 15 amino acids upstream in nearly all Skp1 proteins (28).

In *Dictyostelium*, hydroxylation of Skp1 has been detected based on subsequent recognition and modification by GnT1. In a lysate of a P4H mutant strain (HW288) supplemented with His_6-rP4H1, rGnT1, and UDP-[^{3}H]GlcNAc, Skp1 was the only target that could be detected by radioactive labeling.[2] Analysis of the completely sequenced *Dictyostelium* genome does not yield good candidates for HIFα-type genes,[2] though transcription factors of this type may be obscured by sequence drift considering the long evolutionary distance between *Dictyostelium* and animals. BLAST studies reveal remote candidates for some subunits of the VHL E3 complex,[2] which will require further analysis to validate. Therefore, it is currently difficult to predict whether *Dictyostelium* P4H1 has a function related to that of its animal counterparts. However, it clearly controls the subsequent glycosylation of Skp1 Pro^{143}.

A striking property of P4H1 is its exquisite sensitivity to O_2 levels, with an apparent K_m of 40% O_2. In animals, a similar O_2 dependence has been proposed to function as a primary O_2 sensor for cells to regulate the HIFα-dependent transcription of O_2-sensitive genes such as glycolytic enzymes to support anaerobic metabolism and growth factors that promote hematopoiesis or angiogenesis (24). *Dictyostelium* also exhibits O_2-dependent activities. Cytochrome oxidase subunit VII is encoded by two genes whose expression is oppositely regulated by O_2 tension (60). Culmination, the final morphogenetic step in sporulation, and terminal cell differentiation also require nearly normal O_2 tension (60, 61). The polarity and direction of migrating slugs appear to be influenced by O_2 levels (62). O_2 regulation appears to be a primordial cell function, and the O_2 dependence of P4H1 shown here (Fig. 6*C*) suggests that it may be involved in O_2 sensing in *Dictyostelium*. The two P4H1 mutant strains (HW288 and HW289) have a culmination defect[2] that correlates with the O_2 dependence of this step in normal cells, as if mutant cells cannot detect O_2. In addition to O_2, α-ketoglutarate, ascorbate, and Fe^{2+} have also been proposed to physiologically regulate animal HIFα-type P4Hs (22, 23). The dependence of purified P4H1 on physiological levels of these small metabolic compounds suggests that any of these factors might contribute to the regulation of Skp1 glycosylation in *Dictyostelium* and other microbes in which predicted genes similar to those that modify Skp1 have been found (12).

Acknowledgments—We are grateful to Drs. A. Bochkarev and E. Bochkareva for the gift of plasmids and Dr. Ira Blader for the gift of desferrioxamine.

REFERENCES

1. Cardazo, T., and Pagano, M. (2004) *Nat. Rev. Mol. Cell Biol.* **5,** 739–750
2. Mohanty, S., Lee, S., Yadava, N., Dealy, M. J., Johnson, R. S., and Firtel, R. A. (2001) *Genes Dev.* **15,** 1435–1448
3. Zheng, N., Schulman, B. A., Song, L., Miller, J. J., Jeffrey, P. D., Wang, P., Chu, C., Koepp, D. M., Elledge, S. J., Pagano, M., Conaway, R. C., Conaway, J. W., Harper, J. W., and Pavletich, N. P. (2002) *Nature* **416,** 703–709
4. Cope, G. A., and Deshaies, R. J. (2003) *Cell* **114,** 663–671
5. Seol, J. H., Shevchenko, A., Shevchenko, A., and Deshaies, R. J. (2001) *Nat. Cell Biol.* **3,** 384–391
6. Giot, L., Bader, J. S., Brouwer, C., Chaudhuri, A., Kuang, B., Li, Y., Hao, Y. L., Ooi, C. E., Godwin, B., Vitols, E., Vijayadamodar, G., Pochart, P., Machineni, H., Welsh, M., Kong, Y., Zerhusen, B., Malcolm, R., Varrone, Z., Collis, A., Minto, M., Burgess, S., McDaniel, L., Stimpson, E., Spriggs, F., Williams, J., Neurath, K., Ioime, N., Agee, M., Voss, E., Furtak, K., Renzulli, R., Aanensen, N., Carrolla, S., Bickelhaupt, E., Lazovatsky, Y., DaSilva, A., Zhong, J., Stanyon, C. A., Finley, R. L., White, K. P., Braverman, M., Jarvie, T., Gold, S., Leach, M., Knight, J., Shimkets, R. A., McKenna, M. P., Chant, J., and Rothberg, J. M. (2003) *Science* **302,** 1727–1736
7. Teng-umnuay, P., Morris, H. R., Dell, A., Panico, M., Paxton, T., and West, C. M. (1998) *J. Biol. Chem.* **273,** 18242–18249
8. West, C. M. (2003) *CMLS Cell. Mol. Life Sci.* **60,** 229–240
9. van der Wel, H., Morris, H. R., Panico, M., Paxton, T., Dell, A., Kaplan, L., and West, C. M. (2002) *J. Biol. Chem.* **277,** 46328–46337
10. Wang, F., Metcalf, T. van der Wel H., and West, C. M. (2003) *J. Biol. Chem.* **278,** 51395–51407
11. Ercan, A., and West, C. M. (2005) *Glycobiology*, in press
12. West, C. M., van der Wel, H., Sassi, S., and Gaucher, E. A. (2004) *Biochim. Biophys. Acta* **1673,** 29–44
13. van der Wel, H., Fisher, S. Z., and West, C. M. (2002) *J. Biol. Chem.* **277,** 46527–46534
14. Ketcham, C., Wang, F., Fisher, S. Z., Ercan, A., van der Wel, H., Locke, R. D., Sirajud-Doulah, k., Matta, K. L., and West, C. M. (2004) *J. Biol. Chem.* **279,** 29050–29059
15. Teng-umnuay, P., van der Wel, H., and West, C. M. (1999) *J. Biol. Chem.* **274,** 36392–36402
16. Sassi, S., Sweetinburgh, M., Erogul, J., Zhang, P., Teng-umnuay, P., and West, C. M. (2001) *Glycobiology* **11,** 283–295
17. Myllyharju, J. (2003) *Matrix Biol.* **22,** 15–24
18. Bruick, R. K., and McKnight, S. L. (2001) *Science* **294,** 1337–1340
19. Epstein, A. C., Gleadle, J. M., McNeill, L. A., Hewitson, K. S., O'Rourke, J., Mole, D. R., Mukherji, M., Metzen, E., Wilson, M. I., Dhanda, A., Tian, Y. M., Masson, N., Hamilton, D. L., Jaakkola, P., Barstead, R., Hodgkin, J., Maxwell, P. H., Pugh, C. W., Schofield, C. J., and Ratcliffe, P. J. (2001) *Cell* **107,** 43–54
20. Schofield, C. J., and Ratcliffe, P. J. (2004) *Nat. Rev. Mol. Cell Biol.* **5,** 343–354
21. Lando, D., Gorman, J. J., Whitelaw, M. L., and Peet, D. J. (2003) *Eur. J. Biochem.* **270,** 781–790
22. Knowles, H. J., Raval, R. R., Harris, A. L., and Ratcliffe, P. J. (2003) *Cancer Res.* **63,** 1764–1768
23. Dalgard, C. L., Lu, H., Mohyeldin, A., and Verma, A. (2004) *Biochem. J.* **380,** 419–424
24. Safran, M., and Kaelin, W. G., Jr. (2003) *J. Clin. Investig.* **111,** 779–783
25. Glockner, G., Eichinger, L., Szafranski, K., Pachebat, J. A., Bankier, A. T., Dear, P. H., Lehmann, R., Baumgart, C., Parra, G., Abril, J. F., Guigo, R., Kumpf, K., Tunggal, B., Cox, E., Quail, M. A., Platzer, M., Rosenthal, A., and Noegel, A. A. (2002) *Nature* **418,** 79–85
26. Kivirikko, K. I., and Myllyla, R. (1982) *Methods Enzymol.* **82,** 245–304
27. Hirsila, M., Koivunen, P., Gunzler, V., Kivirikko, K. I., and Myllyharju, J. (2003) *J. Biol. Chem.* **278,** 30772–30780
28. West, C. M., Kozarov, E., and Teng-umnuay, P. (1997) *Gene* (*Amst.*) **200,** 1–10
29. West, C. M., Scott-Ward, T., Teng-umnuay, P., van der Wel, H., Kozarov, E., and Huynh, A. (1996) *J. Biol. Chem.* **271,** 12024–12035
30. van der Wel, H., Morris, H. R., Panico, M., Paxton, T., Dell, A., Thomson, J. M., and West, C. M. (2001) *J. Biol. Chem.* **276,** 33952–33963
31. Puta, F., and Zeng, C. (1998) *Folia Biol.* (*Prague*) **44,** 185–188
32. Thuring, R. W., Sanders, J. P., and Borst, P. (1975) *Anal. Biochem.* **66,** 213–220
33. Zhang, Y., Zhang, P., and West, C. M. (1999) *J. Cell Sci.* **112,** 4367–4377
34. Pang, K. M., Lynes, M. A., and Knecht, D. A. (1999) *Plasmid* **41,** 187–197
35. Kozarov, E., van der Wel, H., Field, M., Gritzali, M., Brown, R. D., and West, C. M. (1995) *J. Biol. Chem.* **270,** 3022–3033
36. Bochkareva, E., Frappier, L., Edwards, A. M., and Bochkarev, A. (1998) *J. Biol. Chem.* **273,** 3932–3936
37. Zhang, Y., Brown, R. D., and West, C. M. (1998) *Biochemistry* **37,** 10766–10779
38. Ivan, M., Haberberger, T., Gervasi, D. C., Michelson, K. S., Gunzler, V., Kondo,

K., Yang, H., Sorokina, I., Conaway, R. C., Conaway, J. W., and Kaelin, W. G., Jr. (2002) *Proc. Natl. Acad. Sci. U. S. A.* **99,** 13459–13464
39. Vervoort, E. B., van Ravestein, A., van Peij, N. N. M. E., Heikoop, J. C., van Haastert, P. J. M., Verheijden, G. F., and Linskens, M. H. K. (2000) *Nucleic Acids Res.* **28,** 2069–2074
40. West, C. M., van der Wel, H., Coutinho, P. M., and Henrissat, B. (2005) in *Dictyostelium Genomics* (Loomis, W. F., and Kuspa, A., eds) pp. 235–264, Horizon Scientific Press, Norfolk, UK
41. Varshavsky, A. (1996) *Proc. Natl. Acad. Sci. U. S. A.* **93,** 12142–12149
42. Vranka, J. A., Sakai, L. Y., and Bachinger, H. P. (2004) *J. Biol. Chem.* **279,** 23615–23621
43. McNeill, L. A., Hewitson, K. S., Gleadle, J. M., Horsfall, L. E., Oldham, N. J., Maxwell, P. H., Pugh, C. W., Ratcliffe, P. J., and Schofield, C. J. (2002) *Bioorg. Med. Chem. Lett.* **12,** 1547–1550
44. Oehme, F., Jonghaus, W., Narouz-Ott, L., Huetter, J., and Flamme, I. (2004) *Anal. Biochem.* **330,** 74–80
45. Tuckerman, J. R., Zhao, Y., Hewitson, K. S., Tian, Y. M., Pugh, C. W., Ratcliffe, P. J., and Mole, D. R. (2004) *FEBS Lett.* **576,** 145–150
46. Ivan, M., Kondo, K., Yang, H., Kim, W., Valiando, J., Ohh, M., Salic, A., Asara, J. M., Lane, W. S., and Kaelin, W. G., Jr. (2001) *Science* **292,** 464–468
47. Hieta, R., Kukkola, L., Permi, P., Pirila, P., Kivirikko, K. I., Kilpelainen, I., and Myllyharju, J. (2003) *J. Biol. Chem.* **278,** 34966–34974
48. Metzen, E., Berchner-Pfannschmidt, U., Stengel, P., Marxsen, J. H., Stolze, I., Klinger, M., Huang, W. Q., Wotlaw, C., Hellwig-Burgel, T., Jelkmann, W., Acker, H., and Fandrey, J. (2003) *J. Cell Sci.* **116,** 1319–1326
49. de Bruin, E. C., Werten, M. W., Laane, C., and de Wolf, F. A. (2002) *FEMS Yeast Res.* **1,** 291–298
50. Eriksson, M., Myllyharju, J., Tu, H., Hellman, M., and Kivirikko, K. I. (1999) *J. Biol. Chem.* **274,** 22131–22134
51. Kaska, D. D., Gunzler, V., Kivirikko, K. I., and Myllyla, R. (1987) *Biochem. J.* **241,** 483–490
52. Hieta, R., and Myllyharju, J. (2002) *J. Biol. Chem.* **277,** 23965–23971
53. Aravind, L., and Koonin, E. V. (2001) *Genome Biology* http://genomebiology.com/2001/2/3/research/0007
54. Pereira, T., Zheng, X., Ruas, J. L., Tanimoto, K., and Poellinger, L. (2003) *J. Biol. Chem.* **278,** 6816–6823
55. Huang, J., Zhao, Q., Mooney, S. M., and Lee, F. S. (2002) *J. Biol. Chem.* **277,** 39792–39800
56. Kuznetsova, A. V., Meller, J., Schnell, P. O., Nash, J. A., Ignacak, M. L., Sanchez, Y., Conaway, J. W., Conaway, R. C., and Czyzyk-Krzeska, M. F. (2003) *Proc. Natl. Acad. Sci. U. S. A.* **100,** 2706–2711
57. Min, J. H., Yang, H., Ivan, M., Gertler, F., Kaelin, W. G., and Pavletich, N. P. (2002) *Science* **296,** 1886–1889
58. Frei, C., and Edgar, B. A. (2004) *Dev. Cell* **6,** 241–251
59. Martin-Puig, S., Temes, E., Olmos, G., Jones, D. R., Aragones, J., and Landazuri, M. O. (2004) *J. Biol. Chem.* **279,** 9504–9511
60. Sandona, D., Gastaldello, S., Rizzuto, R., and Bisson, R. (1995) *J. Biol. Chem.* **270,** 5587–5593
61. Sternfeld, J., and Bonner, J. T. (1977) *Proc. Natl. Acad. Sci. U. S. A.* **74,** 268–271
62. Sternfeld, J., and David, C. N. (1981) *J. Cell Sci.* **50,** 9–17